LBNL-57100

COMPARISON BETWEEN EXPERIMENTS AND CFD PREDICTIONS OF MIXED CONVECTION FLOWS IN AN ATRIUM

B. Jayaraman, E. U. Finlayson, E. E. Wood, T. L. Thatcher, M. D. Sohn,
P. N. Price, R. G. Sextro, A. J. Gadgil

Environmental Energy Technologies Division
Indoor Environment Department
Lawrence Berkeley National Laboratory,
Berkeley, CA 94720, USA

February 2005

This work was supported by the Assistant Secretary for Energy Efficiency and Renewable Energy, Building Technologies Program, through the U.S. Department of Energy, Contract No. DE-AC02-05CH11231.

COMPARISON BETWEEN EXPERIMENTS AND CFD PREDICTIONS OF MIXED CONVECTION FLOWS IN AN ATRIUM

B. Jayaraman*, E. U. Finlayson, E. E. Wood, T. L. Thatcher, M. D. Sohn, P. N. Price, R. G. Sextro, A. J. Gadgil

Indoor Environment Department, Lawrence Berkeley National Laboratory, Berkeley, CA 94720, USA.

ABSTRACT
This paper compares results from a computational fluid dynamics (CFD) simulation of airflow and pollutant dispersion under mixed-convection conditions with experimental data obtained in our 7m x 9m x 11m high experimental facility. A tracer gas was continuously released from a 1 m^2 horizontal source 0.5 m above the floor. Path-integrated concentrations were measured along multiple short and long sampling paths in three horizontal planes. A steady state CFD analysis was used to model these experiments. The Reynolds Averaged Navier-Stokes (RANS) equations were solved for the flow and temperature field using the commercial CFD software, StarCD. CFD results were compared with the measured path-integrated concentrations. Accuracy of CFD predictions was found to improve with inclusion of thermal effects, and further by using a low-Re turbulence model.

INDEX TERMS
Mixed convection, airflow, pollutant dispersion, CFD, large indoor space

INTRODUCTION
Large rooms with mechanically driven flows usually differ from smaller rooms in 3 important ways: (1) larger mixing times (Gadgil et al. 2003), (2) more ventilation inlets and exhausts and (3) stronger buoyancy effects owing to small temperature differences. In the current paper we show that it is important to model the mixed convection effects to predict pollutant transport with acceptable accuracy.

To improve our understanding of airflow and dispersion in large rooms, researchers at Lawrence Berkeley National Lab have conducted tracer gas experiments in an 11 m tall atrium to generate high fidelity measurements and to develop CFD models of concentrations throughout the room (Fischer et al. 1999). We measured path integrated concentration every 7 seconds at multiple locations and heights in the interior of the atrium and obtained high quality data which we believe is unmatched in the published literature. To our knowledge CFD predictions of pollutant transport have not been compared to such quality data in the earlier published literature.

Recently Finlayson et al. (2004) published comparisons of CFD predictions with experiments of pollutant dispersion in a scale model of the same atrium under isothermal conditions, and found very good agreement with experimental data. We now consider non-isothermal conditions, and experimental data from the full-scale atrium.

* Corresponding author email: bjayaraman@lbl.gov

The Rayleigh number, which represents the ratio of buoyancy to viscous forces, can be very high for tall spaces leading to turbulent airflow in the room. Although the standard k-ε model is widely used for most building airflow applications, previous studies (Moser, 1991) have reported difficulties with this model for natural and mixed convection flows.

In the present work, simulations are carried out using two turbulence models for mixed convection flow: (1) the standard k-ε turbulence model and (2) a low-Reynolds number model with hybrid wall functions. An isothermal simulation with standard k-ε model is also carried out to understand the implications of model simplifications on the predictions. We compare the results from these simulations with the experimental data to determine the accuracy of the predictions.

EXPERMENTAL SETUP

The experimental atrium shown in Figure 1a has dimensions of 7m x 9m x 11m high (volume ~690 m^3). A dedicated heating and ventilation (HVAC) system supplies 590 l/s (1250 CFM) of air to the atrium at a temperature of 21^o C (70^o F), through five supply registers that discharge horizontally into the atrium. The exhaust outlet is located on the ceiling. A complete description of the atrium and of the typical experimental setup can be found in Fischer (1999).

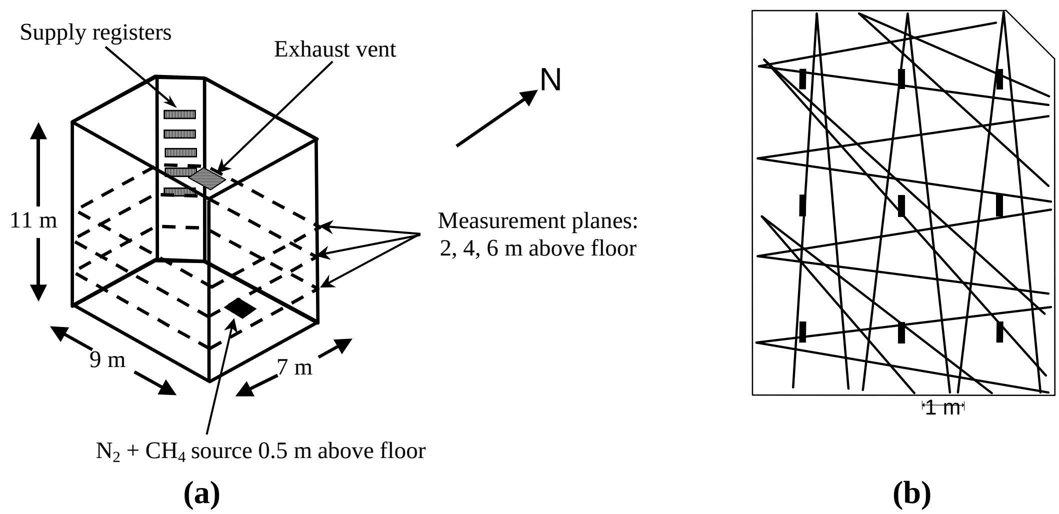

Figure 1a: *3-D view of the experimental atrium showing locations of air supply and exhaust vents, tracer gas release location, and tracer gas measurement heights*

Figure 1b: *Plan view of the optical path geometry for the measurement plane at 2m above the floor. Thin lines indicate ray paths of the ten long-path sensors. A first-surface mirror at the vertex of each path reflects the IR ray to the detector. The thick lines indicate ray paths of nine short-path sensors*

Mixed convection conditions exist in the atrium due to the combination of natural convection due to temperature differences between the walls, and forced convection due to mechanically driven airflow from the HVAC system. Temperature sensors placed on the walls collected data at five-minute intervals. Each wall had 3 to 4 temperature sensors arrayed approximately every 2 m vertically.

Several experiments were carried out in this atrium. In the experiment that we discuss in this paper, we released 4% methane in nitrogen continuously from a 1m^2 area located 0.5 m above the floor, at 0.5 l/s (1.06 CFM). The HVAC system provided the only outside air into the atrium, and there was no recirculation. We measured path-integrated concentrations every seven seconds using infra-red absorption along several short (0.5 m) and long (2-10 m) paths at three heights (Figure 1a). Figure 1b shows the short and long paths in the lowest measurement plane, z=2m, and are similar to measurement paths at z=4m and z=6m. The lower two measurement planes are below the lowest air supply registers. We simulate the experiment during a period when the airflow conditions are fully developed and path-integrated concentrations are stable.

CFD MODEL

The computational mesh consists of approximately 190,000 cells. In the core of the grid the cells have dimensions of 0.12m x 0.17m x 0.1m. The mesh is aligned with the flow direction near the supply registers, to in order to minimize numerical diffusion. Spatial discretization is carried out using the Monotone Advection and Reconstruction Scheme (MARS), a second-order scheme (Asproulis 1994) that suppresses numerical diffusion. We obtained the steady-state airflow and temperature fields by solving the Reynolds Averaged Navier-Stokes equations (RANS) using the commercial CFD software, StarCD. The system of equations are iteratively solved using the algebraic multigrid (AMG) method with a modified predictor-corrector SIMPLE algorithm and pseudo transient time marching with a time step of 0.05 sec. We used a turbulent Schmidt number of 0.6 based on findings from our earlier work (Finlayson 2004).

The CFD simulation cases and the modelling assumptions are presented in Table 1.

Table 1: *Simulated test cases*

Test case	Model Assumptions	Boundary Conditions
A	Isothermal, Standard k-ε	All walls and air at the same temperature
B	Non-isothermal, Standard k-ε	Each wall at uniform temperature
C	Non-isothermal, Low-Re model	Each wall at uniform temperature

The airflow and temperature computations are considered converged when the cumulative normalized residual for all the flow variables dropped below 10^{-3}. The dilute methane tracer is treated as a neutrally buoyant scalar. The steady-state concentration field is obtained by solving the scalar mass transport equation. We terminated the tracer gas concentration calculations when the cumulative normalized residual of the mass transport equation dropped below 10^{-7}.

RESULTS AND DISCUSSION

In the experiment the HVAC-supplied air is approximately 2^{o} C hotter than the walls. The average surface temperature distribution is summarized in Table 2.

Table 2: *Average surface temperature*

Wall	**Temperature ^{o}C**
South	18.9
North	19.2
West	17.2
East	18.5
Floor	19.8
Ceiling	18.2

The non-isothermal CFD simulations show the inlet jets coalescing and rising towards the ceiling. These simulations also show a stable stratification of temperature in the chamber. The tracer gas is released in the cold part of the atrium at 0.5m above the floor. The path integrated concentration data along the long and short paths provide the basis for comparing the three CFD simulations with experiment, as described below. We consider the CFD predictions to agree well with the data, if the model and experimental results are within a factor of two (Finlayson 2004).

CASE A: ISOTHERMAL SIMULATION

We carried out an isothermal simulation to examine the effect of ignoring the thermal effects. Path-averaged concentration predictions along the various paths on three measurement planes are compared with the measured data in Figure 3. The horizontal lines in the figure indicate the 80% interquantile range of the data during the period of interest. The isothermal model severely under-predicts the tracer gas concentrations in the lower and middle planes along all the long paths, and most of the short paths. All but one of the concentration predictions for the paths in the upper plane fall within a factor of two, showing a good agreement with the data. In this case the upper plane is located in a region where mechanical mixing is dominant, so assuming isothermal conditions does not appear to severely degrade the predictions. Overall, these results show that the isothermal model does not adequately predict concentrations in the regions where temperature effects influence the flow.

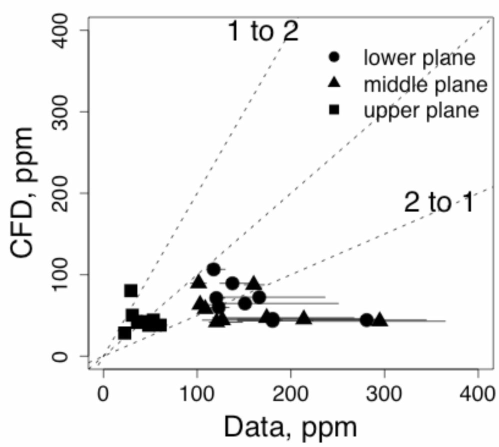

(a)

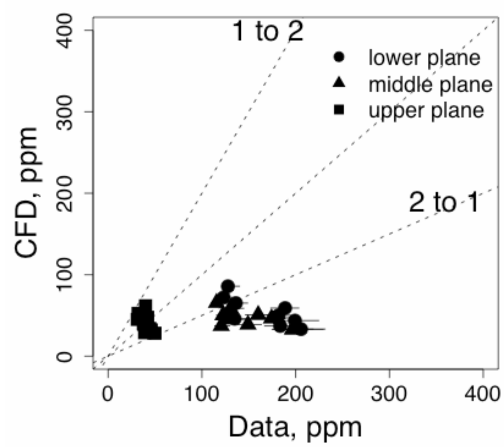

(b)

***Figure 3**. Comparison of path-averaged concentrations measured experimentally and predicted by the Case A CFD along (a) short and (b) long paths*

CASE B: NON-ISOTHERMAL SIMULATION WITH STANDARD k-ε MODEL

In this case, the steady-state airflow and temperature fields are obtained using a standard k-ε turbulence model. Since the MARS second-order scheme led to convergence difficulties, the simulation is carried out using the first-order upwind differencing scheme.

As can be seen from Figure 4, the average concentrations along the short and long paths in the lower plane are consistently over-predicted. Four of the nine short-path predictions (Figure 4a) in the lower plane fall outside the plotting range and are too high compared to data.

The long-path predictions for the lower plane (Figure 4a) are somewhat over-predicted compared to the data, although all but two are within a factor of two when considering the

80% interquantile range of the experimental data. The middle plane predictions for the short paths show a spread in the values, although all are within a factor of two when the range in the measured values is taken into account. For the long paths, the middle plane predictions are within a factor of two of the experimental data. The predictions corresponding to the upper plane fall within the factor of two region for both short and long paths.

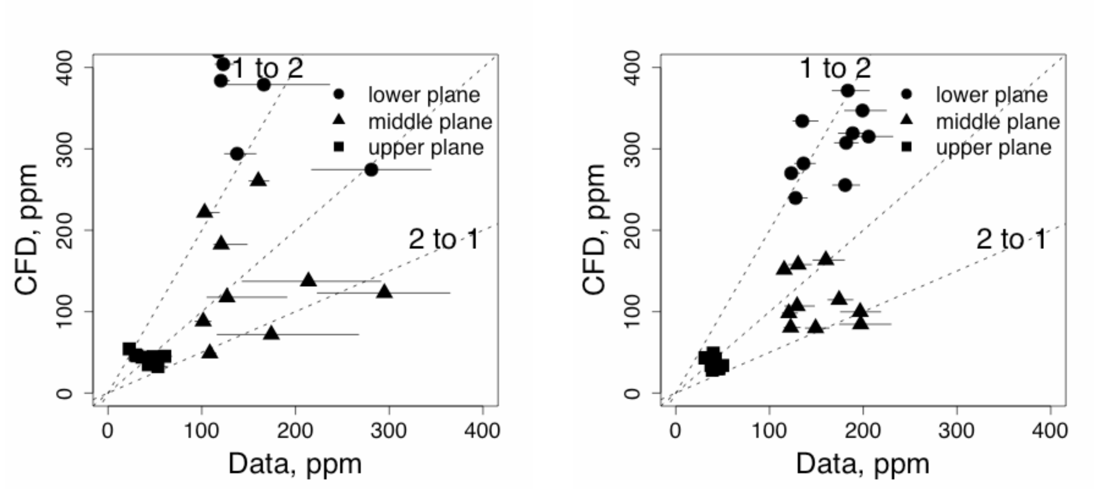

(a) (b)

Figure 4: *Comparison of path-averaged concentrations measured experimentally and predicted by the Case B CFD along (a) short and (b) long paths*

CASE C: NON-ISOTHERMAL SIMULATION WITH LOW-RE MODEL

Lastly, we performed a simulation using a low-Reynolds-number turbulence model with hybrid wall functions (Adapco 2004). The hybrid wall function uses a special wall boundary condition that eliminates the requirement of $y^+ = 1$ close to the wall, resulting in a reduction of computational cost. Local mesh refinement is carried out normal to the walls. The refined mesh has roughly 280,000 cells, resulting in a maximum y^+ of 9.8 near the wall. The mesh resolution in the core is the same as for the previous models. Simulations are carried out using both first-order and second-order discretization schemes. We found that the MARS second-order scheme improved the predictions compared to first-order upwind algorithm.

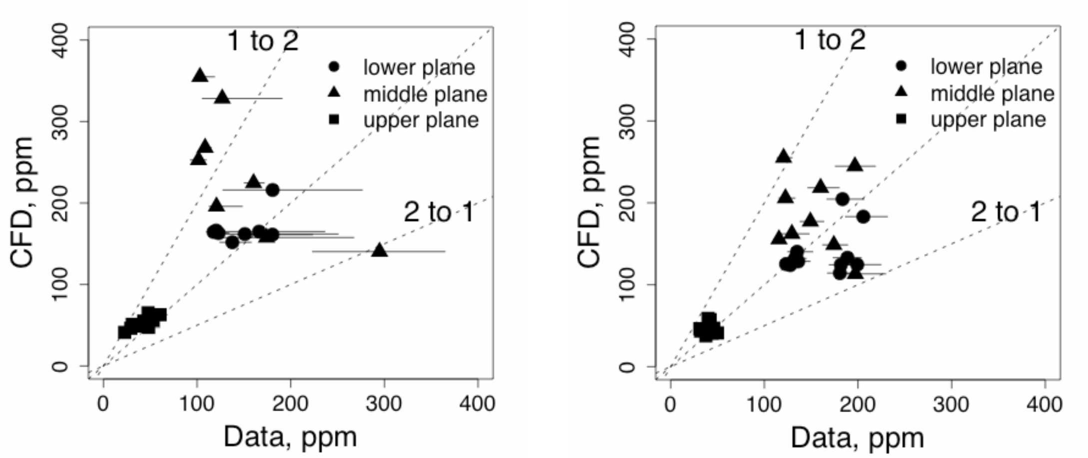

(a) (b)

Figure 5: *Comparison of path-averaged concentrations measured experimentally and predicted by the Case C CFD along (a) short and (b) long paths.*

Figure 5 shows that the low-Reynolds-number model using the second-order scheme results in improved prediction in the lower and the middle planes, compared to standard k-ε model predictions (Case B, Figure 4). Predictions for one short path (Figure 5a) each from the lower and middle planes are too high and are out of plotting range. Significant improvements can be seen in the long-path predictions (Figure 5b), where the predictions for all three planes are within a factor of two of the measured values. The low-Re turbulence model accounts for low-Reynolds-number effects that give better predictions in the low velocity regions and hence yield improved concentration predictions for the lower and middle planes.

CONCLUSION

The present study shows a comparison between detailed, high quality measurements of contaminant dispersion in an atrium and the corresponding predictions from three CFD models. The flow and dispersion experiments in this space were conducted under mixed convection conditions. Poor agreement was obtained with an isothermal CFD model. Somewhat better predictions were obtained with a standard k-ε model. The low-Re turbulence model with the MARS second order scheme resulted in the best agreement with the experimental data for all the three measurement planes.

ACKNOWLEDGEMENTS

The authors acknowledge John Rogers and Scott Wilensky of CD-adapco for their help with StarCD. This work was performed under the U.S. Department of Energy Contract No. DE-AC02-05CH11231.

REFERENCES

Adapco 2004. " StarCD Version 3.20: Methodology," *CD adapco group*

Asproulis PN. 1994. "High resolution numerical predictions of hypersonic flows on unstructured meshes," *Ph.D Dissertation, Imperial College, Dept. of Aeronautics, London, England*

Finlayson EU, Gadgil AJ, Thatcher TL and Sextro RG. 2004. "Pollutant dispersion in a large indoor space: Computational Fluid Dynamics (CFD) predictions and comparisons with a scale model experiment for isothermal flow," *Indoor Air* 14(4): 272-283

Fisher ML, Price PN, Thatcher TL, Schwalbe AS, Craig JM, Wood EE, Sextro RG and Gadgil AG. 2001. "Rapid measurement and mapping of tracer gas concentrations in a large indoor space," *Atmospheric Environment*. 35: 2837-2844

Gadgil AJ, Lobscheid C, Abadie MO and Finlayson EU. 2003. "Indoor pollutant mixing time in an isothermal closed room: an investigation using CFD," *Atmospheric Environment* 37:5577-5586

Moser A. 1991. "The message of Annex 20: Air flow patterns within buildings," *Proc. 12th AIVC conference,* Air Movement and Ventilation Control within Buildings